Effect of first tempering temperature on the amount of reversed and retained austenite in Virgo™38, a 16Cr-4Ni low-carbon super-martensitic stainless steel

Gayton Clément[1, 2], *Bosch Cédric*[1], *Rozinoer Alexia*[2], *Millet François*[2], *Wolski Krzysztof*[1], *Stolarz Jacques*[1]

1- École Nationale Supérieure des Mines de Saint-Étienne, SMS center, MPI department, 158 cours Fauriel CS 62362 42023 Saint-Étienne, France

2- General Electric Oil & Gas Thermodyn SAS, 480 Allée Gustave Eiffel, 71200 Le Creusot, France

Keywords

Supermartensitic stainless steel, Retained austenite, Tempering, Hydrogen charging

Summary

Within this work, the influence of the tempering treatments on the microstructure of a 16Cr-4Ni low-carbon supermartensitic stainless steel (SMSS) was studied. The work was focused on the determination of the presence and the amount of reverted austenite (austenite formed during tempering) and of retained austenite (austenite stable at room temperature) . Different samples, initially coming from the same ingot, were treated in order to obtain different retained austenite contents. Microstructures obtained were hydrogen charged by cathodic polarization in NaCl solution. The amount of hydrogen trapped in these microstructures was measured by high temperature outgassing using thermal desorption spectroscopy, and was correlated to the amount of retained austenite measured by X-ray diffraction (XRD).

Context

The Virgo™38, a 16Cr-4Ni low-carbon supermartensitic stainless steel (SMSS), is an alternative of the well-known AISI410. Compared with AISI410, it exhibits better ductility and corrosion resistance [1], combined with high mechanical resistance. Its properties lead it to be used, among others, for the construction of centrifugal compressor's impellers working in sour environments rich in CO_2 and H_2S. To be safely used, this alloy has to fulfil strict requirement described in the NACE standard MR0175 – ISO15156 [2]. The targeted microstructure of Virgo™38 is composed of tempered α' martensite containing retained austenite γ_r in sufficient but not too high volume fraction and located between martensitic laths. The principal role of retained austenite is to improve fracture toughness of the material. After austenitization at high temperature (>1000°C), the alloy is quenched in oil to room temperature. To ensure that no retained austenite subsists after quenching, a sub-zero treatment is applied. Two-stage tempering is then carried out slightly above the Ac1 temperature in order to form the targeted fraction of reverted austenite. The role of second tempering, applied according to NACE guidelines at a slightly lower temperature than the first one, is to transform fresh martensite which is likely to form in the first tempering stage. After double tempering, the retained austenite fraction is expected to be around 30%. Furthermore, double tempering is supposed to increase austenite stability with respect to plastic deformation induced martensitic transformation [3].

1 Introduction

Supermartensitic stainless steels are currently used with success for oil & gas applications. Nevertheless, some failures have recently occurred during service in sour environments [4]. In order to improve corrosion properties and prevent any failure, one has to better understand the influence of metallurgy and mechanics on hydrogen assisted cracking.

As solubility and diffusion coefficients within austenite and martensite are not the same (see Table 1) [5] [6], the distribution of hydrogen within the steel is supposed to be heterogeneous, austenite playing the role of hydrogen tank. Hence, the higher the amount of retained austenite, the higher the amount of trapped hydrogen.

Table 1: Diffusion coefficients and solubility of hydrogen in different phases of steels

	Ferrite α	Martensite α'	Austenite γ
Diffusion coefficient at 25°C (in cm²/s)	~ 10^{-4}	~ 10^{-6}	~ 10^{-12}
Solubility at 20°C (in wt. ppm)	~ 10^{-4}	~ 10^{-3}	~ 10^{-1}

Furthermore, as previously mentioned, retained austenite fraction depends on the tempering temperature. Starting from a purely martensitic state (after quenching), tempering is carried out above Ac1. Austenite forms along prior austenite grain boundaries and martensitic interlath boundaries [7]. When tempering temperature increases, the amount of martensite transformed into austenite (reverted austenite γ_{rev}) increases as well, however a part of it transforms back into fresh martensite (α') on cooling, so that the final austenite content after tempering (retained austenite γ_r) is smaller than γ_{rev}. During tempering, nickel tends to diffuse into austenite grains [8] so that its average concentration within this phase depends on its volume fraction. Since the stability of reverted austenite depends on its average Ni content, relative to its effect on Ac1 and M_s, the final amount of retained austenite is indirectly function of tempering temperature. For this reason, a maximum of reverted austenite is supposed to be observed for an intermediate tempering temperature depending on the composition of the steel [8].

The current sequence of heat treatment, according to NACE requirements [2] is shown in Figure 1. On this schematic representation, γ_{rev} and γ_r correspond to reverted and retained austenite respectively while α' and α'' correspond to fresh and tempered martensite respectively. δ represents δ-ferrite, potentially present in supermartensitic steels.

Furthermore, austenite stability at room temperature may be seriously affected in presence of stresses (applied and/or residual), in particular when they induce plastic strains. The martensitic transformation occurring in such conditions, called Strain Induced Martensitic Transformation (SIMT) also depends on austenite composition and it is well documented for different types of stainless steels [3] [8] [9] [10] [11]. For example, Smirnova et al. [11] showed that, in a 13Cr supermartensitic stainless steel, the austenite fraction drops from 19% down to 3% before and after 0.4% tensile strain (corresponding to the yield strength).

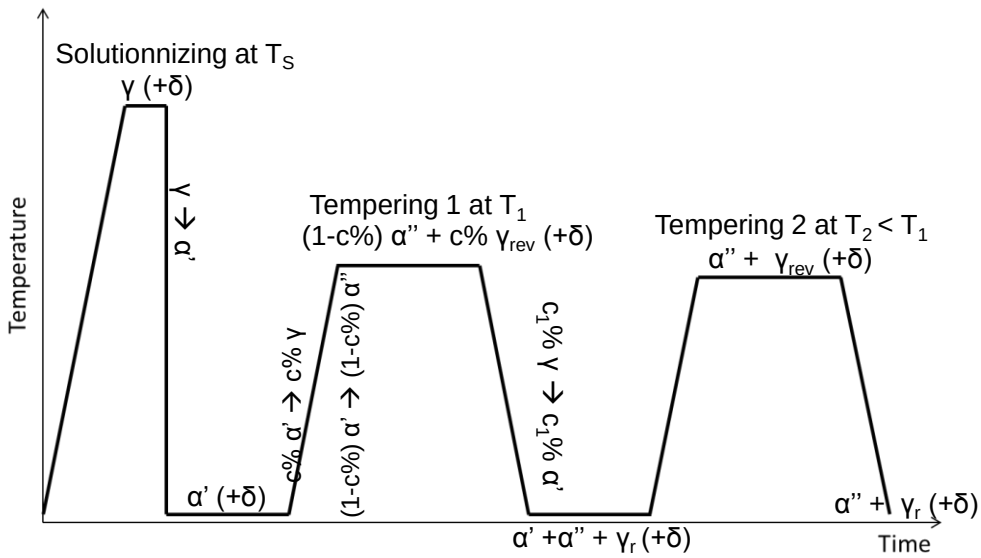

Figure 1: Thermal profile including expected phases at each step, corresponding to the NACE standards

According to Chan et al. [12], the difference between the diffusion coefficients and the solubility of hydrogen in both phases, martensite and austenite, contributes to localise hydrogen trapping during diffusion at the interfaces between austenite and martensite (Figure 2). In this way, cracking is favoured along the austenite/martensite interfaces.

Moreover, hydrogen can modify the stability of retained austenite and be rejected on the phase transformation forehead during austenite's transformation (SIMT), or be in supersaturation into the martensitic phase after SIMT, causing possible embrittlement.

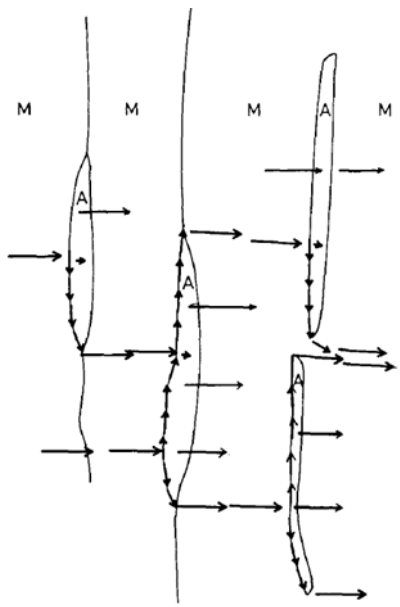

Figure 2: Hydrogen diffusion path and trapping in martensitic stainless steels containing retained austenite [12]

The goal of the present study is to establish a relation between the retained austenite fraction and the amount of hydrogen that can be stored inside the material. The second purpose is to study the stability of austenite with plastic deformation.

2 Material and experimental methods

For this work, an industrial heat of Virgo™38 transformed by Forgia Rapida Srl with a composition indicated in Table 2 was chosen.

Table 2: Chemical composition and mechanical properties of the Virgo™38 studied

C (wt.%)	Cr (wt.%)	Ni (wt.%)	Mn (wt.%)	YS (MPa)	UTS (MPa)	HRC
0.045	15.31	4.64	0.71	690	880	26

After sub-zero oil quenching, tempering at temperatures between 580°C and 660°C was carried out (Table 3) in order to obtain microstructures with different volume fractions of retained austenite. The retained austenite fractions were measured using a Panalytical X'Pert diffractometer. The volume fraction of each phase was then determined by the Rietveld method [13] [14] using the free software MAUD. This technique does not require external calibration and can measure the austenite content with good precision insofar as retained austenite content is greater than 2%. This technique can be used because the samples have no preferential texture after tempering as determined by XRD. A strict procedure of metallographic preparation was applied in order to ensure that no SIMT occurs at the sample surface during preparation.

Table 3: Heat treatments performed

Specimen	Temperature of austenitization	Quenching	Tempering 1
A	1020°C, 15min	Oil quenching + sub-zero treatment in nitrogen, 5min	580°C, 2h
B			590°C, 2h
C			600°C, 2h
D			610°C, 2h
E			620°C, 2h
F			630°C, 2h
G			640°C, 2h
H			650°C, 2h
I			660°C, 2h

As expected after quenching in nitrogen, the resulting microstructures are all purely martensitic.

Several samples were hydrogen charged by cathodic polarization during 10 days in a 30g/L NaCl solution deaerated with N_2 at a potential of -1200mV. Before charging, the samples were polished in order to remove the oxide layer formed during previous heat treatments which can act as a diffusion barrier. As previously mentioned, the polishing procedure prevents any austenite transformation through SIMT in the superficial layer of specimen. The amount of hydrogen stored in the different microstructures is then determined by thermal desorption analysis with a spectrometer between room temperature and 900°C. Samples were heated at 20°C/min.

Reverted austenite fractions were measured during tempering by in-situ X-ray diffraction analysis inside a HTK16 furnace. Specific samples with a 300µm thick were used.

In order to check the mechanical stability of retained austenite, tensile tests at a strain rate of 10^{-4} s^{-1} were performed until failure on the specimen. Retained austenite fractions have been measured before and after the test, on the fracture surface.

3 Results and discussion

Before studying microstructures developed in lab using different tempering treatment, the as received material was investigated. The optical microscopy after Villela's etching and EBSD map presented in Figure 3 show that the microstructure resulting of the thermal treatment according to Figure 1 is composed of martensitic laths with retained austenite inserted between laths. Isolated δ-ferrite grains are also present.

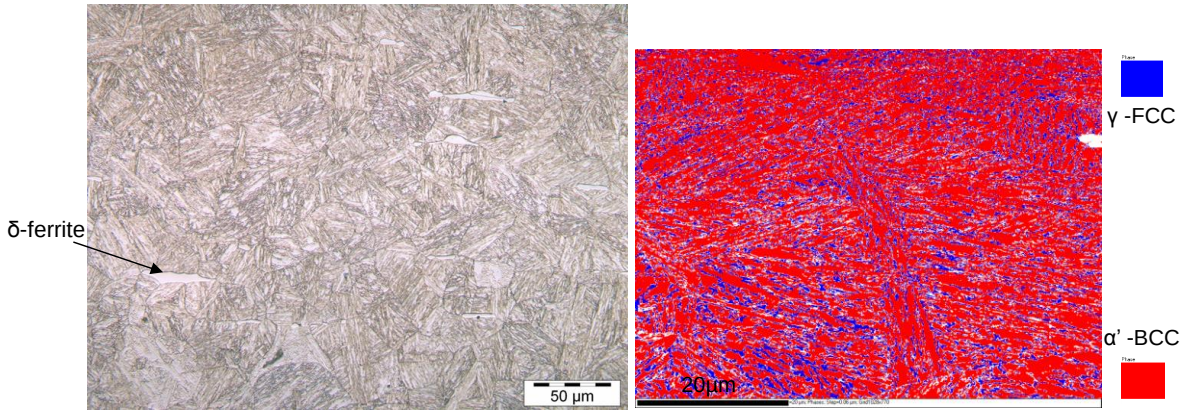

Figure 3: Optical microscopy (Villela's etching) and EBSD map of industrial material

Comparatively, the microstructure obtained after austenitization and sub-zero treatment in nitrogen is presented in Figure 4.

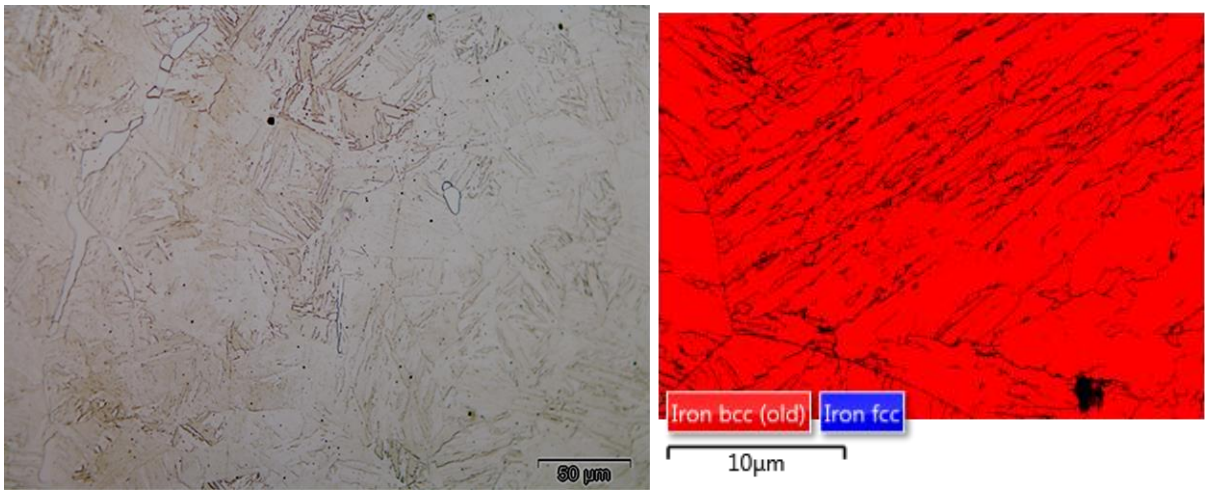

Figure 4: Optical microscopy (Villela's etching) and EBSD map of quenched + sub-zero treated microstructure

In order to determine the phase composition of the sub-zero quenched material, X-ray diffraction analysis was performed (Figure 5).

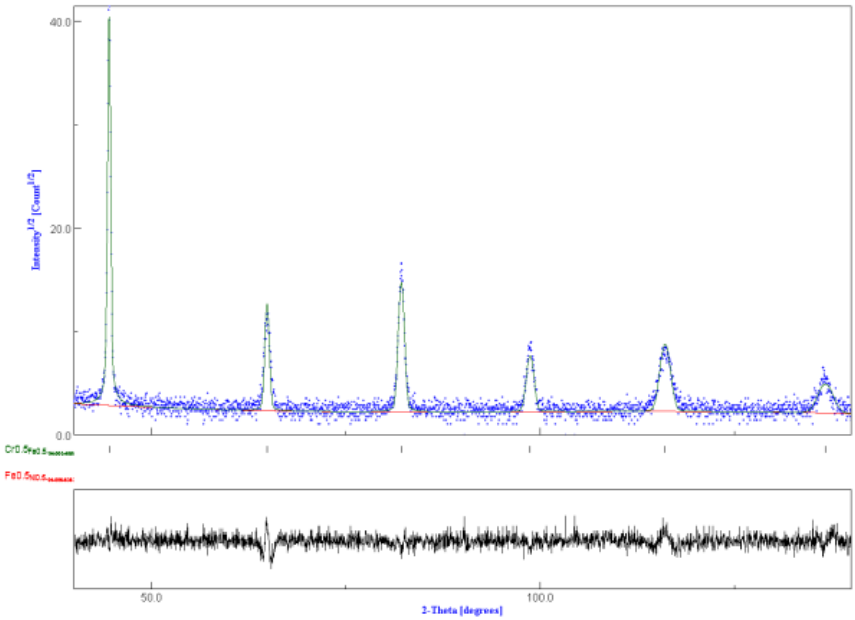

Figure 5: Diffractogram measured on quenched + sub-zero treated samples

No austenitic peaks appear on the diffractogram, which indicates that retained austenite fraction is low, at least under the detection limit (<2%).

The temperatures of phase transitions were measured by dilatometry (Figure 6).

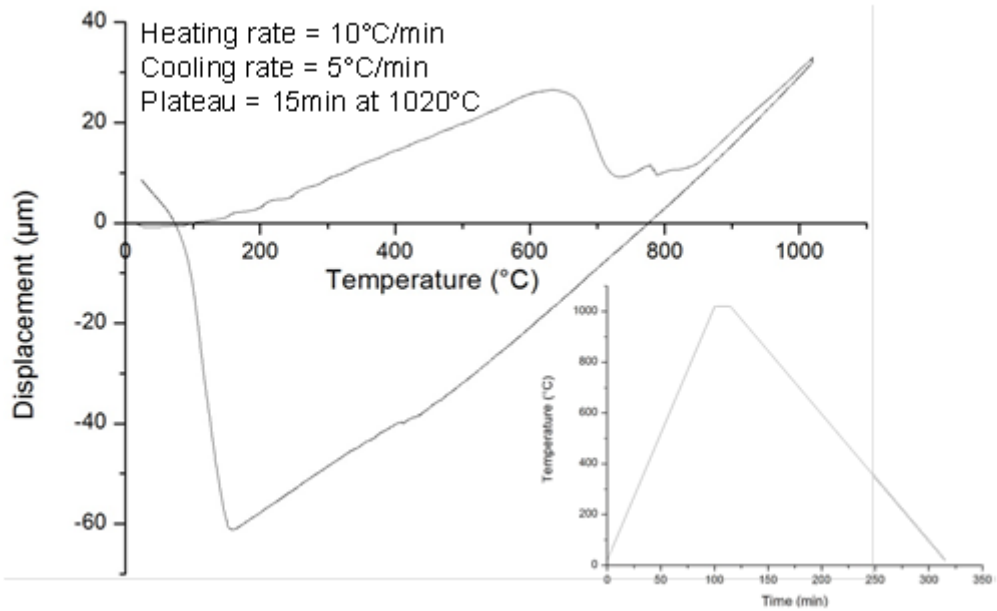

Figure 6: Dilatometric diagram of Virgo™38

This diagram indicates that Ac1≈620°C, Ms≈165°C and Mf<0°C. The latter justify the necessity of a sub-zero treatment after austenitization in order to obtain a fully martensitic structure. A_{c1} and M_S are in accordance with the values given by formulas [15] [16]:

$$Ac1\ (°C) = 850 - 1500(C+N) - 50Ni - 25Mn + 25Si + 25Mo + 20(Cr-10) \approx 610°C$$

$$Ms\ (°C) = 540 - 497C - 6.3Mn - 36.3Ni - 10.8Cr - 46.6Mo \approx 175°C$$

After quenching and sub-zero treatments, samples are tempered at different temperatures as indicated in Table 3. The resulting retained austenite fractions are presented in Figure 7.

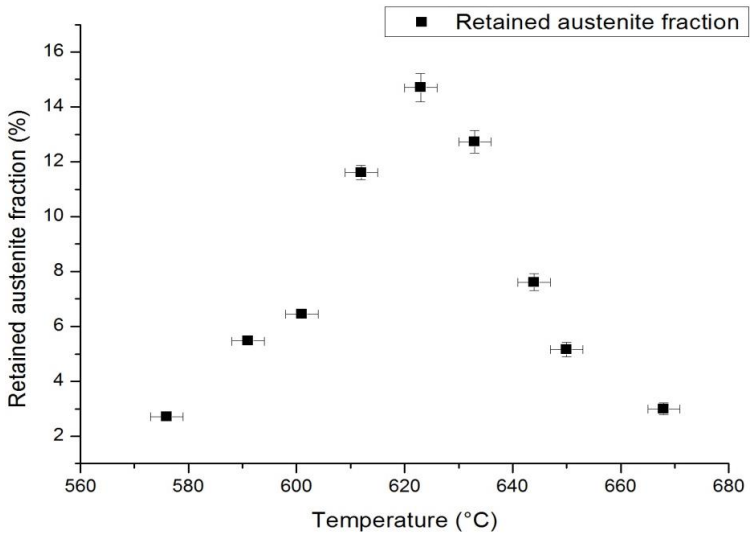

Figure 7: Retained austenite fraction as a function of tempering temperature

One can see that retained austenite fraction depends on tempering temperature, the maximum being reached for treatment at 620°C. At T<620°C, the retained austenite fraction increases when the temperature increases. However, right to the maximum, the retained austenite fraction decreases with increasing tempering temperature, which means that a part of austenite is no more stable. Indeed, austenite stability depends on its composition and during tempering, Ni and Mn tend to diffuse into austenite grains which stabilize it [17]. Obviously, when temperature increases, higher amounts of austenite are formed (Figure 8) and the resulting concentrations of austenite stabilizing elements in austenite grains are lower [8].

The reverted austenite fractions were measured through in situ DRX measurements inside a HTK16 furnace. Results obtained are presented in Figure 8.

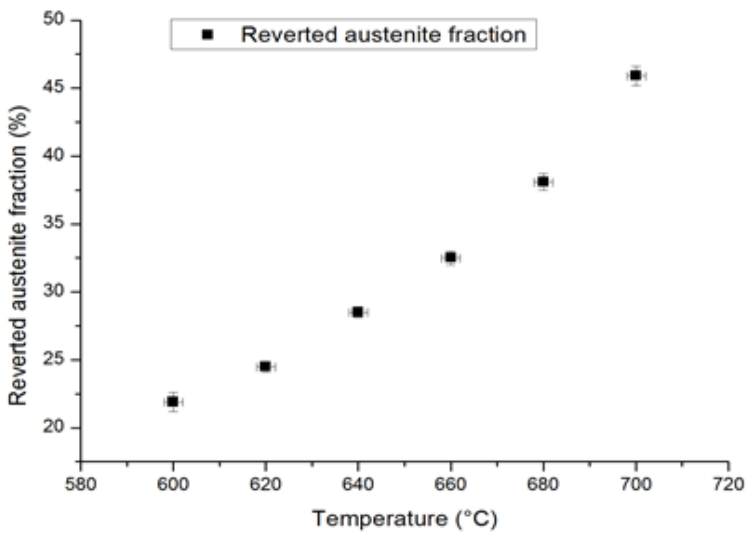

Figure 8: Reverted austenite fraction as a function of tempering temperature

Unlike the retained austenite fraction, the reverted austenite fraction increases continuously when tempering temperature increases. That indicates that during the first tempering fresh martensite is formed during cooling, at least at T>620°C which justi-

fies the second tempering treatment. One can also notice that at high temperature (higher than the temperature producing the maximum retained austenite) a higher fraction of fresh martensite is formed because the difference between retained and reverted austenite fractions is larger.

Once different microstructures have been obtained, some samples have been charged in hydrogen by cathodic polarization according to the procedure described in the previous part. The variation of TDS signal intensity between two samples having respectively 3 % and 15% of retained austenite shows an increase of hydrogen desorbed by TDS in the case where austenite content is higher.

Even if only two microstructures were analysed, one can suppose that the hydrogen concentration increases with the retained austenite fraction which tends to indicate that retained austenite plays the role of hydrogen tank.

Furthermore, the mechanical stability of retained austenite was studied on the industrial material (heat treated according to Figure 1). The retained austenite fraction was determined by XRD before and after a tensile test up to failure at 10^{-4} s^{-1}. It reveals that austenite fraction is below the detection threshold (<2%) after failure (Table 4).

Table 4: Retained austenite fractions measured by XRD before and after failure on the industrial material

	Retained austenite fraction (%)
Before tensile test	22.28 ± 0.36
After failure (measured on fracture surface with parallel slots)	<2%

One can thus see that, in addition to be a hydrogen tank, retained austenite is also sensitive to Strain Induced Martensitic Transformation (SIMT).

4 Conclusions and perspectives

The present study helps understanding the metallurgy of Virgo™38 SMSS after tempering treatment at different temperatures. Beyond a critical temperature, close to 620°C, the retained austenite fraction decreases with increasing tempering temperature, which means that austenite is not stable on subsequent cooling. Moreover, even for the standard heat treatment, retained austenite is not stable under applied stress, so that microstructure is likely to evolve in service with potential consequences on mechanical properties, in particular the fracture toughness.

TDS measurements provide first data on the influence of retained austenite on the hydrogen content of the steel after cathodic charging. As expected, retained austenite plays the role of hydrogen tank. Further investigations will be carried out in order to understand the behaviour of hydrogen trapped inside retained austenite during its transformation into fresh martensite.

During this work, only the effect of the first tempering treatment was investigated. For further conclusions, it is necessary to study the role of the second tempering treatment. Furthermore, the amount of hydrogen trapped in the different microstructures will be quantified.

5 References

[1] H. J. Niedereau, “A new low-carbon 16Cr-5Ni stainless martensitic cast steel,” in *Stainless Steel Castings, ASTM STP 756, V. G. Behal and A. S. Melilli Eds. , American Society for Testing and Materials*, 1982, pp. 382–393.

[2] “Petroleum and natural gas industries - materials for use in H2S containing environments in oil and gas production,” *North Am. Corros. Eng.*

[3] P. Wang, N. Xiao, S. Lu, D. Li, and Y. Li, “Investigation of the mechanical stability of reversed austenite in 13%Cr–4%Ni martensitic stainless steel during the uniaxial tensile test,” *Mater. Sci. Eng. A*, vol. 586, pp. 292–300, Dec. 2013.

[4] T. Cassagne, M. Bonis, C. Duret, and J. L. Crolet, “Limitations of 17-4 PH Metallurgical, Mechanical and Corrosion Aspects.” NACE International.

[5] A. Brass, J. Chene, and L. Coudreuse, “Fragilisation des aciers par l’hydrogène : mécanismes,” *Tech. l’ingénieur M176*, 2000.

[6] G. Hinds, J. Zhao, A. J. Griffiths, and A. Turnbull, “Hydrogen Diffusion in Super 13% Chromium Martensitic Stainless Steel,” *Corrosion*, vol. 61, no. 4, pp. 348–354, 2005.

[7] M. De Sanctis, R. Valentini, G. Lovicu, A. Dimatteo, R. Ishak, U. Migliaccio, R. Montanari, and E. Pietrangeli, “Microstructural Evolution during Tempering of 16Cr-5Ni Stainless Steel: Effects on Final Mechanical Properties,” *Mater. Sci. Forum*, vol. 762, no. 2013, pp. 176–182, Jul. 2013.

[8] Y.-K. Lee, H.-C. Shin, D.-S. Leem, J.-Y. Choi, W. Jin, and C.-S. Choi, “Reverse transformation mechanism of martensite to austenite and amount of retained austenite after reverse transformation in Fe-3Si-13Cr-7Ni (wt-%) martensitic stainless steel,” *Mater. Sci. Technol.*, vol. 19, no. 3, pp. 393–398, Mar. 2003.

[9] D. Thibault, P. Bocher, M. Thomas, J. Lanteigne, P. Hovington, and P. Robichaud, “Reformed austenite transformation during fatigue crack propagation of 13%Cr–4%Ni stainless steel,” *Mater. Sci. Eng. A*, vol. 528, no. 21, pp. 6519–6526, Aug. 2011.

[10] K. G. Solheim, J. K. Solberg, J. Walmsley, F. Rosenqvist, and T. H. Bjørnå, “The role of retained austenite in hydrogen embrittlement of supermartensitic stainless steel,” *Eng. Fail. Anal.*, vol. 34, pp. 140–149, Dec. 2013.

[11] A. Smirnova, “Effect of tensile stress on hydrogen permeation in 13 % Cr super martensitic stainless steel.” pp. 1–12, 2010.

[12] S. L. I. Chan, H. L. Lee, and J. R. Yang, “Effect of Retained Austenite on the Hydrogen Content and Effective Diffusivity of Martensitic Structure,” no. November, pp. 2579–2586, 1991.

[13] R. A. Young, *The Rietveld method*. Oxford: Oxford University Press, 1993.

[14] C. F. Jatczak, J. A. Larson, and S. W. Shin, “Retained austenite and its measurement by X-ray diffraction,” 1980.

[15] A. W. Marshall and J. C. M. Farrar, “Welding of ferritic and martensitic 13%Cr steels: Preliminary report,” *IIW Doc.IX-H-422-98*.

[16] T. G. Gooch, P. Woollin, and Haynes A., “Welding metallurgy of low carbon 13%chromium martensitic steels,” in *Supermartensitic Stainless Steel*, 1999.

[17] G. F. Lovicu, M. De Sanctis, R. Valentini, A. Dimatteo, R. Ishak, U. Migliaccio, R. Montanari, and E. Pietrangeli, “Influence of presence and stability of reverted austenite on mechanical properties of 16Cr-5Ni supermartensitic stainless steel after tempering treatment,” *La metallurgia italianja n°9*, 2013.